

Temperature-dependent pseudogaps in colossal magnetoresistive oxides

T. Saitoh* and D. S. Dessau

Department of Physics, University of Colorado, Boulder, Colorado 80309-0390

Y. Moritomo† and T. Kimura

Joint Research Center for Atom Technology, Tsukuba, Ibaraki 305-0046, Japan

Y. Tokura

*Joint Research Center for Atom Technology, Tsukuba, Ibaraki 305-0046, Japan
and Department of Applied Physics, University of Tokyo, Tokyo 113-0033, Japan*

N. Hamada‡

Joint Research Center for Atom Technology, Tsukuba, Ibaraki 305-0046, Japan

(Received 15 November 1999)

Direct electronic structure measurements of a variety of colossal magnetoresistive (CMR) oxides show the presence of a pseudogap at the Fermi energy E_F which drastically suppresses the electron spectral function at E_F . The pseudogap is a strong function of the layer number of the samples (sample dimensionality) and is strongly temperature dependent, with the changes beginning at the ferromagnetic transition temperature T_c . These trends are consistent with the major transport trends of the CMR oxides, implying a direct relationship between the pseudogap and transport, including the ‘‘colossal’’ conductivity changes which occur across T_c . The k dependence of the temperature-dependent effects indicates that the pseudogap observed in these compounds is not due to the extrinsic effects proposed by Joynt.

The colossal magnetoresistance (CMR) effect recently discovered in the manganese oxides [$\text{La}_{1-x}\text{B}_x\text{MnO}_3$ ($\text{B} = \text{Sr, Ca, Ba}$) and $\text{La}_{2-2x}\text{Sr}_{1+2x}\text{Mn}_2\text{O}_7$] is a phenomenon which dramatically displays a strong correlation between magnetism and electronic conduction.^{1,2} At low temperatures (T), properly doped manganese oxides exhibit ferromagnetic metallic behavior, while at high T they exhibit paramagnetic insulating behavior. If one starts at T slightly above T_c , the application of a magnetic field can play a similar role as T by driving the material through the insulator-metal transition. This is the CMR effect.

Traditionally, the starting point for understanding the electronic and magnetic properties of the CMR oxides is the double-exchange (DE) model originally studied by Zener,³ de Gennes,³ and Anderson and Hasegawa.³ DE says that the hopping probability t for an e_g symmetry (conduction) electron to hop from one site to the next is $t = t_0 \cos(\theta/2)$, where t_0 is the bare hopping probability and θ is the relative angle between two core (t_{2g}) spins (see Fig. 1). A ferromagnetically ordered sample has $\theta = 0$ and so a full hopping probability, while an antiferromagnetically ordered sample has $\theta = 180^\circ$ and no probability of hopping. The paramagnetic case corresponding to $T > T_c$ can be approximated by $\theta = 90^\circ$; i.e., t should be reduced to $\cos(90^\circ/2)$ or about 70% of its original value. A calculation of the bandwidth (W) change with temperature is done more precisely by Kubo,⁴ with the result being very similar to our simple explanation. Directly associated with the change in hopping probability is the effect on the E vs k relations and $N(E_F)$, which is schematically illustrated in Figs. 1(B) and 1(C).⁴ The roughly 30% changes in t and W expected across the transition will contribute to similar changes in the electronic mobility μ and

conductivity σ . Since the conductivity changes across the transition may be many orders of magnitude instead of just a 30% effect [see Fig. 6(B) and Ref. 2], it has been argued that additional physics must be necessary to explain the conductivity changes in the manganites.^{5,6} The results presented here confirm these ideas but go one further, indicating that at least for the layered samples, DE is probably not even the dominant mechanism but is instead supplements some other more important physics.

We performed angle-resolved photoemission (ARPES) experiments on cleaved single-crystalline samples of layered and pseudocubic manganites at the Stanford Synchrotron Radiation Laboratory (SSRL) using a 50 mm hemispherical analyzer. The energy resolution was about 40 meV full width at half maximum (FWHM) and the k resolution was better than $\pm 0.05\pi$ in the first Brillouin zone at the photon energy of 22.4 eV. The samples were grown by the floating-zone method.^{2,7} The surfaces of the layered samples were mirror-like and high-quality low-energy electron diffraction patterns were easily obtainable, with no evidence of extra superlattice spots. Other indications of the quality of the surfaces are the large amount of E vs k dispersion observed and the T dependence, which as we will see has many similarities to the Drude part of optical conductivity measurements whose probing depth is typically several thousands of Å.⁸ We note that the recent claim that the surface magnetism of the manganites is different from that of the bulk⁹ is on strained thin films which have undergone a complicated surface cleaning procedure. We worry that these films may have a nonideal surface, which is further confirmed by a lack of E vs k dispersion from these surfaces. The nearly two-dimensional structure of the layered manganites as well as the very large

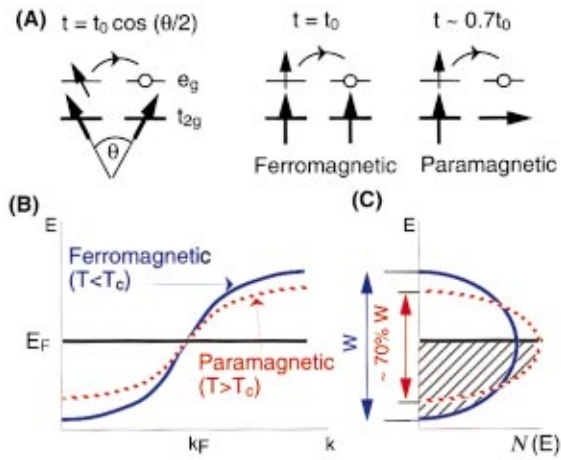


FIG. 1. (Color) (A) The relevant Mn-O derived electronic orbitals for the manganites. According to DE theory t from one site to the next is a strong function of the relative angle (θ) between the t_{2g} spins on the two sites. (B) Schematic drawing of the E vs k relations expected within DE theory. The paramagnetic states should have a dispersion about 70% of that in the ferromagnetic state. (C) Total electronic density of states $N(E)$ expected within DE theory. Concomitant with the reduced dispersion and band-width, the paramagnetic phase is expected to have a slightly higher $N(E)$ at E_F .

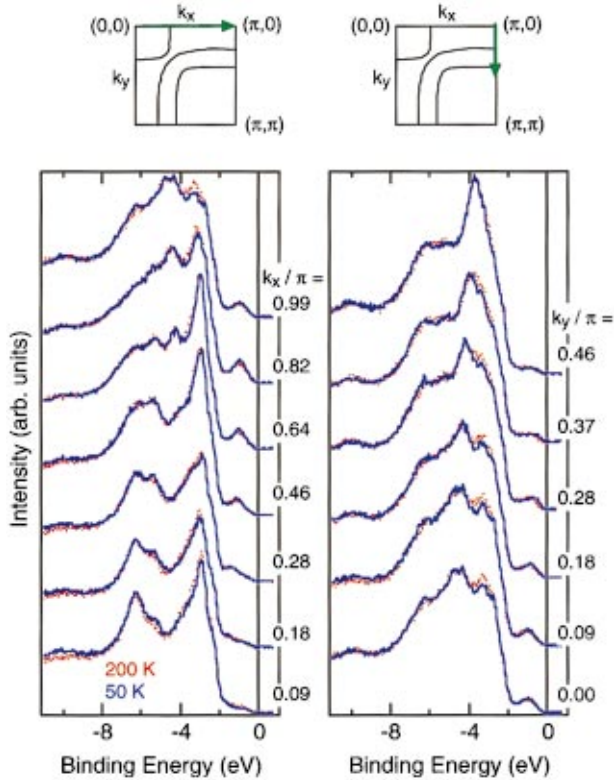


FIG. 2. (Color) ARPES spectra from $h\nu=22.4$ eV of the full valence-band region from $\text{La}_{1.2}\text{Sr}_{1.8}\text{Mn}_2\text{O}_7$ along the $(0,0)$ - $(\pi,0)$ (left panel) and $(\pi,0)$ - (π,π) (right panel) symmetry lines at 200 K (red) and 50 K (blue). The square panels at top show the location of the cuts in one quadrant of the two-dimensional Brillouin zone.

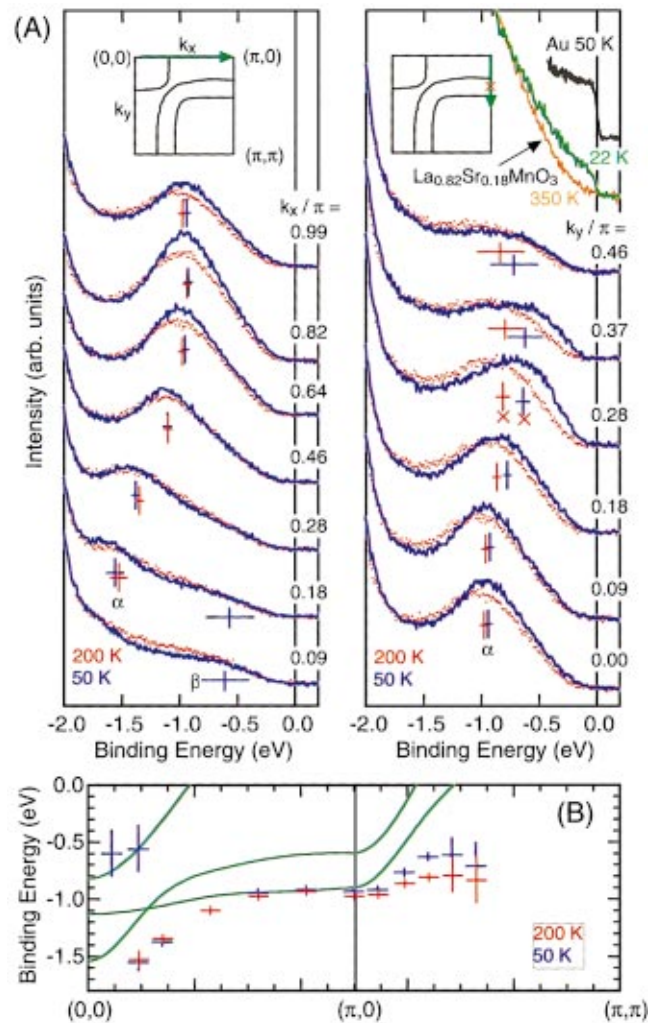


FIG. 3. (Color) (A) Near- E_F spectra taken under identical conditions as the spectra of Fig. 2. The red \times shows the predicted FS crossing point. In the right panel, the $\text{La}_{0.82}\text{Sr}_{0.18}\text{MnO}_3$ spectra at two T and the gold spectrum are shown. (B) Comparison between the experimental dispersion of $\text{La}_{1.2}\text{Sr}_{1.8}\text{Mn}_2\text{O}_7$ from panel (A) (red, 200 K; blue, 50 K) and the LSDA+ U bands (green).

(two-order-of-magnitude) in-plane to out-of-plane transport anisotropy² gives added confidence that the cleaved surfaces measured in our experiments yields electronic structure data representative of the bulk physics of these materials.

Figure 2 shows the full valence band spectra of $\text{La}_{1.2}\text{Sr}_{1.8}\text{Mn}_2\text{O}_7$ along the $(0,0)$ - $(\pi,0)$ - (π,π) symmetry line at 200 K (paramagnetic state) and at 50 K (ferromagnetic state). Figure 3(A) shows the near- E_F data from the same sample taken under identical conditions. All the spectra have been normalized by the total area of the main valence-band spectra at the highest T at each k -space point. The procedure for the angle-integrated spectra of cubic compounds is the same. All 200 K data were taken first, immediately after the sample cleave which was also performed at 200 K. At each emission angle the valence band and near- E_F spectra were taken concurrently without a sample reoptimization or realignment. After all 200 K data were finished the sample was cooled to 50 K and the measurement procedure was repeated. Therefore the low-temperature spectra are more aged than the high-temperature spectra, accounting for the slightly

higher (but still very small) ‘‘dirt’’ peak at -10 eV observed in the low-temperature spectra. We note that with continued aging the dirt peak continues to grow and the emission intensity near E_F is found to decrease. The fact that our low-temperature spectra show the same or even more weight than our high-temperature spectra implies that the temperature-dependent reduction in the spectral weight at high temperatures discussed here is not due to an aging effect. We also checked the reproducibility of the T -dependent changes by several cleaves including warming runs and have confirmed that the qualitative changes were much larger than the aging effects.

Figure 3(A) shows two major features, labeled α and β , the centroids of which are plotted as a function of k in Fig. 3(B) which also includes the $e_{g\uparrow}$ bands from our LSDA+ U band structure calculations.¹⁰ According to the calculation as well as our polarization-dependent photoemission experiments,¹¹ α has primarily $d_{x^2-y^2\uparrow}$ symmetry and β has primarily $d_{3z^2-r^2\uparrow}$ symmetry. We see that the dispersion and energy position of the centroids of the ARPES features is in relatively good agreement with the calculations except near E_F , where a pseudogap suppresses the weight at E_F . Additionally, the experiment shows a k -space locus of lowest-energy excitations forming a large ‘‘ghost’’ Fermi surface (FS),¹⁰ which is in rough agreement with the FS calculated by the local spin density approximation (LSDA) band theory. This large hole FS is also consistent with recent Hall effect measurements.¹²

Joynt has recently argued that the pseudogap observed in photoemission experiments in manganites and possibly many other compounds may be due to extrinsic loss effects.¹³ It is important that we can exclude this possibility before analyzing our data in more detail. In Joynt’s proposal, the electric field created by the outgoing photoelectron produces Ohmic losses, lowering the kinetic energy of the ejected photoelectron. This would show up in the spectra as a pseudogap, even if there was not one in the true density of states, and should be most important for highly resistive samples.

The data of Fig. 3(A) can directly address this question. Some of the curves [for example, $\vec{k}=(\pi,0.28\pi)$] show a significant shift away from E_F with temperature, while other curves [for example, $\vec{k}=(0.46\pi,0)$] show a minimal effect. The minimal temperature-dependent changes observed at $(0.46\pi,0)$ put an upper limit on the magnitude of the effects that could be due to Joynt’s extrinsic losses, and so the dramatic changes observed at $\vec{k}=(\pi,0.28\pi)$ should be of intrinsic origin. Additionally, since there is no effect at some angles from a two-order of magnitude change of resistivity, it should also be clear that the weaker pseudogap observed at $(\pi,0.28\pi)$ at 50 K in the spectra is not due to Ohmic losses [the pseudogap should be measured at the k where the peak is closest to E_F , which occurs at $(\pi,0.28\pi)$]. In a recent Comment and Reply,^{14,15} Joynt agrees that the spectral weight suppression in these compounds appears to be intrinsic.

We discuss two main aspects of the T dependence of the data of Figs. 2 and 3: (1) The data show only a very small change in W , in contradiction with the DE prediction. (2)

There are large changes in the spectral intensity at E_F for k near $(\pi,0.28\pi)$, which are due to the opening of a pseudogap.

(1) DE tells us that W should decrease by about 30% when going from the ferromagnetic to the paramagnetic phases (see Fig. 1). In our measurement, the highest binding energy occupied states that are clearly resolvable are at $(0.18\pi,0)$ and a binding energy near 1.6 eV. Upon going to the high- T paramagnetic state, DE theory predicts that these states should show a significant ($\sim 30\%$) energy shift towards E_F ; i.e., they should appear centered around 1.1 eV. Instead, we observe a small energy shift of approximately 0.06 eV or a change in W of just a few percent ($0.06/1.5=4\%$). This lack of a change in W should imply that a short-range (in-plane) ferromagnetic correlation still exists above T_c . This is consistent with a recent neutron scattering measurement from the same sample source which showed in-plane short-range ferromagnetic order as high as $T=284$ K.¹⁶

(2) In contrast to the small T -dependent changes at $(0.18\pi,0)$, there are dramatic T dependences near $k=(\pi,0.28\pi)$, which corresponds to a predicted FS crossing point as well as the point of closest approach of the peak centroid to E_F . The spectra at the higher T are pushed farther away from E_F and the spectral intensity near E_F is reduced. This behavior represents the opening of a (pseudo)gap centered at E_F with T . In particular, a gap centered at E_F is expected to affect the states near k_F strongly and those away from k_F much more weakly, as observed in our data. We call this gap a pseudogap because the edges of the gap are ‘‘soft’’ and because the spectral weight at E_F is not always completely suppressed.

We note that even at low T the spectra at $(\pi,0.28\pi)$ remain pulled back from E_F , and the spectral weight reaching E_F is vanishingly small. This indicates that the pseudogap is active at low as well as at high T , although it is stronger at high T . Figure 4(A) shows this T dependence in more detail from a different $\text{La}_{1.2}\text{Sr}_{1.8}\text{Mn}_2\text{O}_7$ sample, also measured while cooling. The triangles indicate the spectral weight found very near E_F obtained over two different energy integration windows, and the diamonds show the energy shift of the leading edge (at two different positions on the edge) as a function of T . It is seen that both the near- E_F weight and the position of the leading edge begin increasing at T_c and then rise monotonically without saturation as the T is lowered.

Figure 4(B) shows that a similar T -dependent behavior is found for the perovskite samples, although this time the T_c is very different and we plot the angle-integrated density of states (DOS).¹⁷ As in Figs. 2 and 3, the high-temperature data were measured prior to the low-temperature data, negating the possibility that the trends observed here are due to aging. A portion of the raw data is shown in the upper right hand corner of Fig. 3(A), with similar raw data being presented by other groups.^{18,19} The high- T data do not exhibit any weight right at E_F , while the low T data exhibit a clear Fermi-edge cutoff, indicating a finite DOS at E_F .

The left vertical scale of Fig. 4(B) corresponds to the ratio of the observed weight to the weight deduced from the band structure calculations.²⁰ The way in which this ratio was determined is shown more clearly in Fig. 5, which shows a

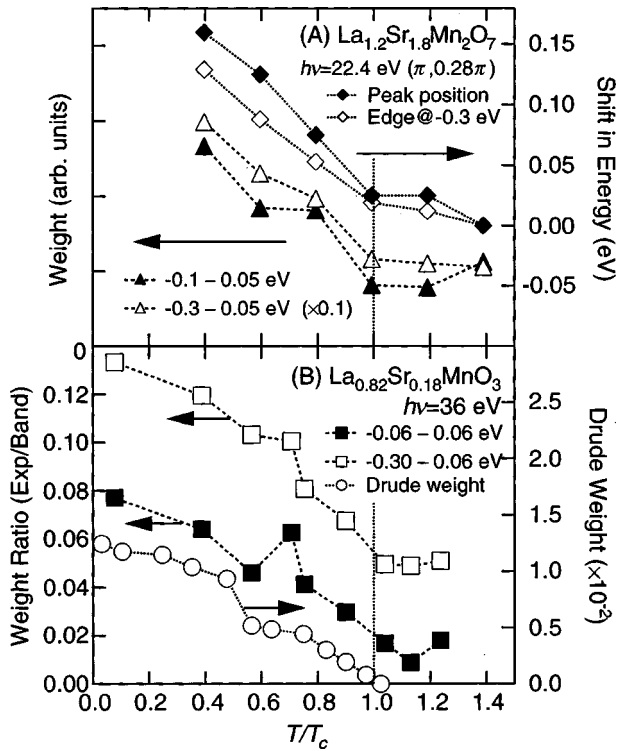


FIG. 4. (A) Integrated spectral weight of $\text{La}_{1.2}\text{Sr}_{1.8}\text{Mn}_2\text{O}_7$ in two different windows and relative energy shifts of the peak and the edge at -0.3 eV at $(\pi, 0.28\pi)$. (B) Comparison of the integrated spectral weight of $\text{La}_{0.82}\text{Sr}_{0.18}\text{MnO}_3$ in two different windows between the experimental spectra and the band structure calculations (Ref. 20). The Drude weight of $x=0.175$ sample (Ref. 8) is also shown for comparison.

comparison of low-temperature (22 K) experimental angle-integrated valence band data to a photoionization cross-section-weighted band structure density of states.²¹ To make this comparison, a small ($\sim 15\%$) background due to inelastically scattered electrons was removed from the experimental photoemission data, and the integrated spectral area under the two curves from 0 to 8 eV was made to match.

While the agreement between the theory and experiment is nowhere very good, it is worst near E_F , where the experiment shows a greatly reduced weight compared to theory. The left axis of Fig. 4 shows that the near- E_F weight always

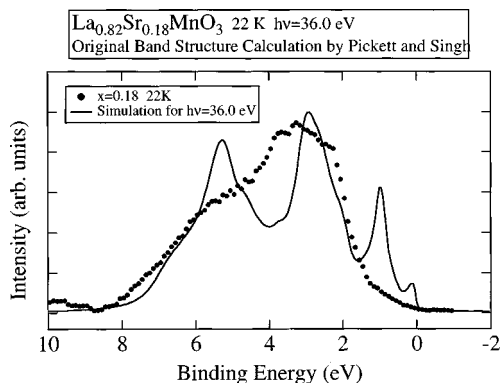


FIG. 5. Angle-integrated valence band data from $\text{La}_{0.82}\text{Sr}_{0.18}\text{MnO}_3$ (filled circles) versus the cross section corrected band structure density of states, courtesy of W. Pickett (line).

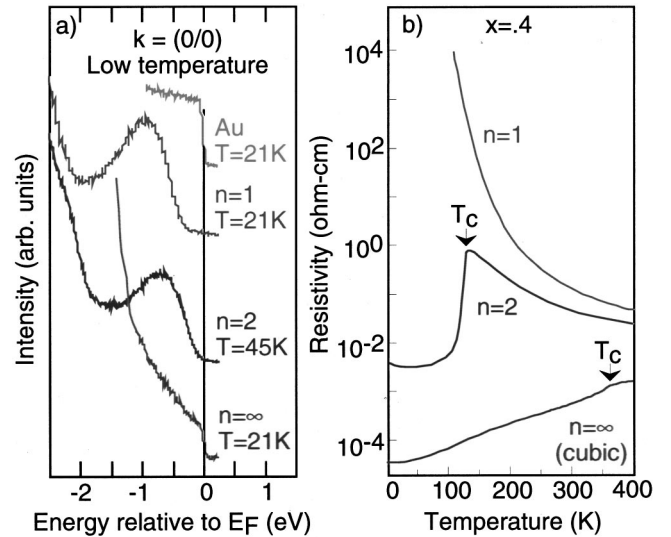


FIG. 6. (A) Normal emission photoemission data in the near E_F region for the layered ($n=1,2$) and cubic ($n=\infty$) systems, all with doping $x=0.4$. For the layered samples, this k point mostly samples the $d_{3z^2-r^2}$ out-of-plane bands (β in Fig. 2). The photon energy was 48 eV for $n=1,2$ and 36 eV for $n=\infty$ and for Au. At these high photon energies these states have a higher cross section than shown in Fig. 2. Spectra taken at k near $(\pi, 0.28\pi)$ show a similar layer-number dependence (not shown). (B) Resistivity as a function of T for the same samples (Ref. 2).

remains at least a factor of 10 lower than the predicted weight, even at the lowest T , even though a clear Fermi edge is observed in the perovskite spectrum of Fig. 3(A). As shown in the figure, a similar T dependence and reduction in low-frequency spectral weight is observed in the Drude portion of optical conductivity experiments of a very similar ($x=0.175$) sample.⁸

Figure 6 shows near- E_F photoemission data and dc resistivity from the three different families of the manganites, all with the same doping level of 0.4 holes per Mn site. At the low T of the measurements, the cubic sample has a finite $N(E_F)$ and is metallic, and the $n=1$ sample has a clear gap and is insulating [$n=1$ samples are insulating for all doping levels and T (Ref. 22)], while the $n=2$ sample has a vanishingly small weight at E_F and is barely metallic. The trends in the data again indicate the significance of the pseudogap in explaining the transport properties of the manganites. Our data indicate a direct and possibly causal relationship between $N(E_F)$ and conductivity σ . Considering the very small bandwidth W changes that are observed across T_c , it appears that the changes in $N(E_F)$ due to the pseudogap are more important for the metal-insulator transition than is the DE effect.

It may be tempting to attribute the decrease in spectral weight at E_F to be due to a decrease in mobile carriers. For instance, on the basis of transport measurements Jaime and Salamon have proposed a two-fluid model where the reduced conductivity of the manganites is due to a T -dependent reduction in the number of otherwise normal high-mobility carriers.²³ Such a situation should lead to a small FS with normal (i.e., nongapped) behavior. Here, we have a large ‘‘ghost’’ FS enclosing a large number of carriers,¹⁰ although each of these carriers gives a drastically reduced spectral

weight at E_F due to the pseudogap. The large size of this observed ghost FS is consistent with the recent Hall effect experiments which indicated a large FS.¹²

A few theoretical works are able to predict gaps or pseudogaps in the electron spectral function. In particular, the Jahn-Teller (JT) effect has been heavily discussed in the context of the manganites. Strong coupling between the electrons and the JT phonons will break the degeneracy of the e_g orbitals, opening a gap between them.^{5,24} However, E_F will only lie in this gap for a doping level of $x=0$, i.e., for d^4 compounds such as LaMnO_3 . Our work clearly shows that there is a gap at E_F for filling levels far away from $x=0$, so coupling to Jahn-Teller phonons cannot explain the pseudogap. The inclusion of other phonons such as breathing-mode phonons may be relevant,⁵ although it is unclear if the electron-phonon coupling to these modes can be strong enough to open a gap as large as what we have experimentally observed. If so, then the pseudogap as well as the broad ARPES peaks may be explainable within the context of strong electron-phonon coupling.¹⁰ Other interesting possibilities are the recent works by Alexandrov and Bratkovsky²⁵ and Moreo *et al.*,²⁶ both of which predict the gap to exist at E_F irrespective of the doping level, as observed experimentally. Alexandrov and Bratkovsky's pseudogap is due to the formation of bipolarons, while that of Moreo *et al.* is due to strong electron-phonon coupling in the presence of phase separation. More recently, Ferrari *et al.*²⁸ have explicitly considered the role of the local Coulomb interaction to model the ARPES spectra of the manga-

nites. They observe clear dispersion for states away from E_F and a strong suppression of the spectral weight very near E_F . This suppression is due to the Coulomb interaction (Hubbard gap) and can also qualitatively explain the anomalous suppression of the Drude peak in the optical conductivity experiments. Other effects that should be considered are the charge-orbital ordering tendencies²⁷ as well as long-range Coulomb interactions which may open a Coulomb gap.²⁹

Finally, we briefly contrast the physics between the pseudogap discussed here and the pseudogap in high-temperature superconductors (HTSC's).³⁰ In HTSC's the pseudogap occurs below the temperature T^* and corresponds to a reduced resistance state, while in manganites the pseudogap is most active above the temperature T_c , and corresponds to an increased resistance state. We suggest that this can be understood by assuming that in HTSC's only the spin excitations are gapped, while for manganites the charge excitations are gapped as well. The elucidation of the pseudogap origin will likely be a crucial step in our progress to understand the physics of both of these families of compounds.

We would like to thank A. Andreev, A. Fujimori, T. Katsufuji, A. Millis, T. Mizokawa, C.-H. Park, L. Radzihovsky, and Z.-X. Shen for fruitful discussions and W. E. Pickett for the numerical data of the band structure calculations. This work was supported by an ONR grant and by NEDO. SSRL is operated by the DOE, Office of Basic Energy Sciences.

*Present address: Photon Factory, KEK, Tsukuba 305-0801, Japan.

†Present address: CIRSE, Nagoya University, Nagoya 464-01, Japan.

‡Present address: Science University of Tokyo, Noda 278-8510, Japan.

¹K. Chahara *et al.*, Appl. Phys. Lett. **63**, 1990 (1993); R. von Helmolt *et al.*, Phys. Rev. Lett. **71**, 2331 (1993); Y. Tokura *et al.*, J. Phys. Soc. Jpn. **63**, 3931 (1994).

²Y. Moritomo *et al.*, Nature (London) **380**, 141 (1996).

³C. Zener, Phys. Rev. **82**, 403 (1951); P.-G. de Gennes, *ibid.* **118**, 141 (1960); P.W. Anderson and H. Hasegawa, *ibid.* **100**, 675 (1955).

⁴K. Kubo, J. Phys. Soc. Jpn. **33**, 929 (1972).

⁵A.J. Millis, P.B. Littlewood, and B.I. Shraiman, Phys. Rev. Lett. **74**, 5144 (1995); A.J. Millis, B.I. Shraiman, and R. Mueller, *ibid.* **77**, 175 (1996); A.J. Millis, R. Mueller, and B.I. Shraiman, Phys. Rev. B **54**, 5405 (1996).

⁶H. Röder, J. Zang, and A. Bishop, Phys. Rev. Lett. **76**, 1356 (1996).

⁷A. Urushibara *et al.*, Phys. Rev. B **51**, 14 103 (1995).

⁸Y. Okimoto *et al.*, Phys. Rev. B **55**, 4206 (1997).

⁹J.-H. Park *et al.*, Phys. Rev. Lett. **81**, 1953 (1998).

¹⁰D.S. Dessau *et al.*, Phys. Rev. Lett. **81**, 192 (1998).

¹¹D.S. Dessau *et al.*, in *Science and Technology of Magnetic Oxides*, edited by M.F. Hundley, J.H. Nickel, R. Ramesh, and Y. Tokura, MRS Symposia Proceedings No. 494 (Materials Research Society, Pittsburgh, 1998), p. 181.

¹²A. Asamitsu and Y. Tokura, Phys. Rev. B **58**, 47 (1998).

¹³R. Joynt, Science **284**, 777 (1999).

¹⁴D.S. Dessau and T. Saitoh, Science **287**, 767a (2000).

¹⁵R. Joynt, Science **287**, 767a (2000).

¹⁶T. Perring *et al.*, Phys. Rev. Lett. **80**, 4359 (1998)

¹⁷We have not been able to obtain the mirror-quality cleaves necessary to obtain high-quality ARPES data on the perovskite samples.

¹⁸J.-H. Park *et al.*, Phys. Rev. Lett. **76**, 4215 (1996); **81**, 1953 (1998); Nature (London) **392**, 794 (1998).

¹⁹D.D. Sarma *et al.*, Phys. Rev. B **53**, 6873 (1996).

²⁰W.E. Pickett and D.J. Singh, Phys. Rev. B **53**, 1146 (1996).

²¹The Mn 3d and O 2p partial densities of states from the band theory calculation were each individually weighted by the theoretical cross sections, obtained from J.J. Yeh and I. Lindau, At. Data Nucl. Data Tables **32**, 1 (1985). Following this a slight energy-dependent broadening was applied to the theoretical density of states to simulate lifetime and energy resolution effects.

²²Y. Moritomo *et al.*, Phys. Rev. B **51**, 297 (1995).

²³M. Jaime and M. Salamon (unpublished).

²⁴D.J. Singh *et al.*, Phys. Rev. B **57**, 88 (1998).

²⁵A.S. Alexandrov and A.M. Bratkovsky, Phys. Rev. Lett. **82**, 141 (1999).

²⁶A. Moreo *et al.*, Phys. Rev. Lett. **83**, 2773 (1999).

²⁷S. Ishihara *et al.*, Phys. Rev. B **55**, 8280 (1997).

²⁸V. Ferrari, M.J. Rozenberg, and R. Weht, cond-mat/9906131 (unpublished).

²⁹C.M. Varma, Phys. Rev. B **54**, 7328 (1996).

³⁰A.G. Loeser, Z.-X. Shen, D.S. Dessau, D.S. Marshall, C.-H. Park, P. Fournier, and A. Kapitulnik, Science **273**, 325 (1996); H. Ding, T. Yokoya, J.C. Campuzano, T. Takahashi, M. Randeria, M.R. Norman, T. Mochiku, K. Kadowaki, and J. Giapintzakis, Nature (London) **382**, 51 (1996).